

ORIGINAL ARTICLE

Early inhibition of MMP activity in ischemic rat brain promotes expression of tight junction proteins and angiogenesis during recovery

Yi Yang¹, Jeffrey F Thompson¹, Saeid Taheri², Victor M Salayandia¹, Thera A McAvoy¹, Jeff W Hill¹, Yirong Yang³, Eduardo Y Estrada¹ and Gary A Rosenberg^{1,4,5}

In cerebral ischemia, matrix metalloproteinases (MMPs) have a dual role by acutely disrupting tight junction proteins (TJPs) in the blood–brain barrier (BBB) and chronically promoting angiogenesis. Since TJP remodeling of the neurovascular unit (NVU) is important in recovery and early inhibition of MMPs is neuroprotective, we hypothesized that short-term MMP inhibition would reduce infarct size and promote angiogenesis after ischemia. Adult spontaneously hypertensive rats had a transient middle cerebral artery occlusion with reperfusion. At the onset of ischemia, they received a single dose of the MMP inhibitor, GM6001. They were studied at multiple times up to 4 weeks with immunohistochemistry, biochemistry, and magnetic resonance imaging (MRI). We observed newly formed vessels in peri-infarct regions at 3 weeks after reperfusion. Dynamic contrast-enhanced MRI showed BBB opening in new vessels. Along with the new vessels, pericytes expressed zonula occludens-1 (ZO-1) and MMP-3, astrocytes expressed ZO-1, occludin, and MMP-2, while endothelial cells expressed claudin-5. The GM6001, which reduced tissue loss at 3 to 4 weeks, significantly increased new vessel formation with expression of TJPs and MMPs. Our results show that pericytes and astrocytes act spatiotemporally, contributing to extraendothelial TJP formation, and that MMPs are involved in BBB restoration during recovery. Early MMP inhibition benefits neurovascular remodeling after stroke.

Journal of Cerebral Blood Flow & Metabolism (2013) **33**, 1104–1114; doi:10.1038/jcbfm.2013.56; published online 10 April 2013

Keywords: astrocytes; blood–brain barrier; brain recovery; focal ischemia; matrix proteinases; pericytes angiogenesis

INTRODUCTION

Neurovascular remodeling after stroke has been recently recognized as a promising target for neurologic therapies. Stimulating functional vessel growth may stabilize cerebral perfusion and promote neuronal survival, brain plasticity, and neurologic recovery.¹ During recovery, angiogenesis occurs in the penumbral areas in stroke patients and animals.² Increased microvessel density in penumbral regions after stroke has been observed in humans³ and in animals.^{4,5} Vascular integrity depends on the complex relationship of the tight junction proteins (TJPs) between the endothelial cells, surrounding extracellular matrix, astrocytes, pericytes, and other cells in the neurovascular unit (NVU). In the early stages of angiogenesis, newly formed vessels have increased vascular permeability, suggesting a derangement in TJPs during restoration of the blood–brain barrier (BBB).

In acute ischemia, matrix metalloproteinases (MMPs) open the BBB and cause neuronal death, and MMP inhibitors block TJP breakdown.^{6–9} Furthermore, MMPs are critical for angiogenesis during recovery. Long-term MMP inhibition reduces neuronal plasticity, impairs new vessel formation, and promotes tissue damage in peri-infarct cortex.¹⁰ This suggested that the beneficial

effects of MMP inhibition could be preserved, while the detrimental ones avoided, by limiting their use to the early stages of injury. Therefore, we hypothesized that short-term MMP inhibition could provide the early neuroprotection in NVU and promote angiogenesis.

Earlier we showed that MMP-2 and -9 disrupted the BBB by degrading TJPs, claudin-5 and occludin, within 3 hours of reperfusion.⁹ It is well known that MMPs are critical in angiogenesis, but their role in the eventual remodeling of the NVU has not been studied. Understanding the manner in which the MMPs contribute to the restoration of vascular integrity after several weeks is necessary to plan timing of treatment with MMP inhibitors to avoid interference with the beneficial action of MMPs in angiogenesis.

To investigate the molecular and cellular mechanisms involved in poststroke neurovascular remodeling, we used a rat model of transient middle cerebral artery occlusion (MCAO) with reperfusion. We have chosen spontaneously hypertensive rats because they have clinically relevant risk factors for ischemic stroke.¹¹ We used immunohistochemistry (IHC), western blot, confocal microscopy, and dynamic contrast-enhanced magnetic

¹Department of Neurology, University of New Mexico Health Sciences Center, Albuquerque, New Mexico, USA; ²Department of Radiology and Radiological Sciences, Medical University of South Carolina, Charleston, South Carolina, USA; ³College of Pharmacy, University of New Mexico Health Sciences Center, Albuquerque, New Mexico, USA; ⁴Department of Neurosciences, University of New Mexico Health Sciences Center, Albuquerque, New Mexico, USA and ⁵Department of Cell Biology and Physiology, University of New Mexico Health Sciences Center, Albuquerque, New Mexico, USA. Correspondence: Dr Y Yang, Department of Neurology, MSC11 6035, 1 University of New Mexico, Albuquerque, NM 87131-0001, USA.

E-mail: yyang@salud.unm.edu

This work was supported in part by American Heart Association grants BGIA 0765473Z and BGIA 10BGIA4310034 (to YY), COBRE pilot grant and RAC grant from University of New Mexico (to YY). Confocal images in this paper were generated in the University of New Mexico Cancer Center Fluorescence Microscopy Facility.

Received 3 December 2012; revised 7 March 2013; accepted 14 March 2013; published online 10 April 2013

resonance imaging (MRI) to characterize the role of pericytes, astrocytes, and endothelial cells in the remodeling of TJs and BBB integration. We determined the spatiotemporal involvement of MMP-2 and -3 in the remodeling of TJs in the BBB and migration of new vessels. We report that a single dose of an MMP inhibitor at an early stage in ischemic stroke facilitates later angiogenesis and reduces infarct size at 3 to 4 weeks.

MATERIALS AND METHODS

Middle Cerebral Artery Occlusion with Reperfusion

The study was approved by the University of New Mexico Animal Care Committee and conformed to the National Institutes of Health Guidelines for use of animals in research. Eighty-six male spontaneously hypertensive rats (280 to 300 g of body weight) were subjected to a 90-minute MCAO with reperfusion for 24, and 48 hours, 7 days, and 3 and 4 weeks as previously described.⁸ Thirty-four animals were used in histologic and MRI studies. For the MMP inhibition experiments, groups studied were GM6001 ($n = 26$) and the GM6001-negative control ($n = 26$). The rat numbers did not reflect the rats which died around 12 to 17 days after reperfusion during the long-term studies (33% in control group and 11% in treated group). Inhibition of MMP was performed with a single dose of the broad-spectrum MMP inhibitor, GM6001 (N-[(2R)-2-(Hydroxamidocarbonylmethyl)-4-methylpentanoyl]-L-tryptophan Methylamide; Calbiochem, San Diego, CA, USA) administered immediately before MCAO onset (5 $\mu\text{g}/\text{rat}$, intravenously).¹² Control rats had the same dose of N-t-Butoxycarbonyl-L-leucyl-L-tryptophan Methylamide (Calbiochem), a negative control for GM6001. Both active and inactive drugs were delivered at onset of MCAO. Another group of sham animals ($n = 12$) underwent neck surgery with a suture inserted and rapidly removed.

Immunohistochemistry

Ten micrometer sections from rat brain tissues fixed with 2% paraformaldehyde, 0.1 mol/L sodium periodate, 0.075 mol/L lysine in 100 mmol/L phosphate buffer, pH 7.3 were used for immunohistochemical analysis. Primary antibodies and dilutions used in IHC were claudin-5 (1:500) (Invitrogen, Grand Island, NY, USA), occludin (1:500) (Invitrogen), zonula occludens-1 (ZO-1) (1:200, Invitrogen), MMP-2 (1:300, Chemicon, Temecula, CA, USA), MMP-3 (1:1500, Chemicon), MMP-9 (1:250; Chemicon), VEGF-A (1:1000, Abcam, Cambridge, MA, USA), Ki67 (1:1000, Abcam), RECA1 (1:300, Abcam), glial fibrillary acidic protein (GFAP) (1:400, Sigma-Aldrich, St Louis, MO, USA; 1:100, Abcam), NeuN (1:400; Chemicon), OX-42 (1:400, Accurate) NG2 (1:300, Millipore, Billerica, MA, USA), Desmin (5 $\mu\text{g}/\text{mL}$, Chemicon), PDGFR- β (1:100, Cell Signaling, Danvers, MA, USA).

For immunofluorescence, brain sections were treated with acetone and blocked with 5% normal serum. Primary antibodies were incubated for 24 hours at 4°C. Sections were incubated for 90 minutes at 25°C with secondary antibodies conjugated with FITC or Cy-3 (Jackson Immuno-Research, West Grove, PA, USA) or Cy-5 (Santa Cruz, Santa Cruz, CA, USA). 4'-6-diamidino-2-phenylindole (DAPI) (Molecular Probes, Eugene, OR, USA) was used to label cell nuclei. For brightfield immunolabeling, fixed sections were rehydrated through alcohol series and incubated in phosphate-buffered saline before blocking with 5% normal serum in phosphate-buffered saline. Slides were incubated with Vectastain Elite ABC reagents (Vector Laboratories, Burlingame, CA, USA) and reacted with 3,3'-Diaminobenzidine to allow visualization of immunolabeling and counterstained with cresyl violet acetate (Sigma-Aldrich). The IHC-negative controls were incubated without the primary antibody or with normal (nonimmune) IgGs and no specific immunolabeling was detected (data not shown).

All IHC slides were viewed on an Olympus BX-51 bright field and fluorescence microscope (Olympus America Inc., Center Valley, PA, USA). Dual or triple immunofluorescence slides were also imaged focally to verify colabeling (Zeiss LSM 510; Carl Zeiss Microimaging, Thornwood, NY, USA).

Hematoxylin and Eosin Staining

Paraformaldehyde-fixed tissue sections were assessed for gross tissue damage and hemorrhage by hematoxylin and eosin (H&E) staining using standard techniques using Lillie's variant of Mayer's haemalum (Lillie-Mayer) and eosin/phloxine. Briefly, tissues were rehydrated through

alcohol series and exposed to hematoxylin for nuclear staining. Slides were rinsed in tap water and differentiated using acid alcohol and Scott's tap water substitute. Eosin/phloxine counterstaining was performed followed by serial alcohol dehydration, clearing with xylenes, and coverslipping with DPX. Stained slides were viewed and imaged an Olympus BX-51 bright field microscope equipped with an Optronics digital camera.

Vessel Counting and Tissue Loss Measurement

Rats were killed and perfused for vessel counting at 24 hours, 48 hours, 7 days, and 3 weeks of reperfusion after stroke. Eight brain sections from each animal with an interval of 100 μm covered a span of 800 μm in the peri-Bregma region (~ 1.00 to 0.2 mm rostral to Bregma). Microvessels labeled with RECA-1 were counted in images captured from ischemic hemispheres with a low power objective lens ($4\times$) by using National Institutes of Health Image J. Indicators of animal identity on slides were blinded to the investigator. The number of microvessels was calculated as the mean of the numbers per mm^2 obtained from the imaged sections.

Tissue loss measurement was assessed in 3 week reperused animals. Eight sections per rat with a 100- μm interval (~ 1.00 to 0.2 mm rostral to Bregma) were stained with cresyl violet acetate. Tissue loss was blindly measured in images captured from ischemic hemispheres at low power objective lens ($4\times$) using Image J. The area of tissue loss was calculated as the mean of the mm^2 obtained from eight images.

Western Blots

Western blots were performed to determine protein levels in sham-operated brains, ischemic and nonischemic hemispheres. Proteins were extracted in RIPA buffer. Fifty microgram total proteins were separated on 10% or 12% polyacrylamide gels. The proteins were transferred onto polyvinylidene fluoride membranes. The membranes were then incubated with primary antibodies: claudin-5 (1:500), occludin (1:500), ZO-1 (1:500), VEGF-A (1:2,000), Alk1 (1:1,000, Santa Cruz), Alk5 (1:1,000, Santa Cruz), MMP-2 (1:1,000) and MMP-3 (1:1,000, Epitomics, Burlingame, CA, USA). The membranes were incubated with the respective secondary antibodies and blots were developed using the West Pico Detection System (Pierce, Rockford, IL, USA). Protein bands were visualized on X-ray film. Semiquantitation of target protein intensities was performed with the use of Scion image software (Scion, National Institute of Health, Bethesda, MD, USA), and actin (Sigma-Aldrich) immunoblots on the same polyvinylidene fluoride membranes were used to normalize protein loading and transfer. The results are reported as normalized band intensity for quantifying relative protein expression.

Terminal Deoxynucleotidyl Transferase-Mediated dUTP Nick End Labeling Assay

Terminal deoxynucleotidyl transferase-mediated dUTP nick end labeling (TUNEL) assay was performed to identify the extent of DNA fragmentation and cell death. Using the NeuroTACS II kit (Trevigen, Gaithersburg, MD, USA), brain sections were treated according to manufacturer's procedure. For dual immunofluorescence, brain sections were then exposed to primary antibody and streptavidin fluorescein and prepared as described above. For positive controls, the nuclease provided with the kit was added to the labeling reaction mix and induced TUNEL positivity in all cells. As a negative control, slides were prepared in a labeling reaction mix without the TdT enzyme resulting in no TUNEL positivity (data not shown).

Magnetic Resonance Imaging

For the MRI study, rats at 3 and 4 weeks of reperfusion were transported to the MRI room, placed in a dedicated rat holder, and moved to the isocenter of the magnet before the imaging session. The MRI was performed on a 4.7-T Biospec dedicated research MR scanner (Bruker Biospin, Ettlingen, Germany), equipped with a small-bore linear radio-frequency coil (i.d., 72 mm).¹³ Initial localizer images were acquired followed by T2-weighted and diffusion-weighted images.

The slices containing the lesion were identified from the T2-weighted structural images, and the same slice location was prescribed for all the subsequent magnetic resonance (MR) protocols. Dynamic contrast-enhanced MRI protocol for acquiring data for the Patlak plot modeling method was then implemented. In this acquisition, a reference baseline acquisition using the fast T1 mapping protocol was obtained. Rats were injected with 0.2 mmol/kg gadolinium-diethylenetriaminepentaacetic acid

(molecular mass = 938 Da; Bayer Co, Wayne, NJ, USA) as a bolus into the femoral vein via an indwelling catheter, followed by imaging with rapid T1 mapping protocol, collecting 15 images over 45 minutes. The total scan time was 3 minutes and 20 seconds for each time point. The MR protocol parameters for rapid T1 mapping were optimized for accuracy of T1 relaxation time estimate in a single, normal rat brain (contralateral) before including that animal in the study. Postprocessing of the raw data involved denoising, field correction, and reconstruction of permeability coefficient maps by using Patlak plots modeling. All data processing was performed using in-house software written in 64-bit MATLAB (Mathworks, Natick, MA, USA) running on a UNIX machine. Detailed descriptions of the method were reported previously.¹⁴

Tissue perfusion was measured using the arterial spin labeling (ASL) method. The sequence: FAIR-RARE (Flow-sensitive Alternating Inversion Recovery Rapid Acquisition with Relaxation Enhancement) was used to implement ASL with parameters: echo time (TE)/repetition time (TR) = 46/16,000 ms, field of view = 4 cm × 4 cm, Slice thickness = 1 mm, number of slice = 1, matrix = 128 × 128. Perfusion map was calculated using ASL_Perfusion_Processing macro in ParaVision 5.1 (Bruker Biospin MRI). The principle is as follows: inversion recovery data from the imaging slice are acquired after selective inversion of the slice and after inversion of the slice including the surrounding tissue, containing the supplying arteries. The difference of the inverse of the apparent T1 images then yields a measure of the cerebral blood flow.

Statistical Analysis

Data were analyzed using an unpaired Student's *t*-test (two groups) or one-way analysis of variance with a *post hoc* Student–Newman–Keuls test (multiple comparisons). In all statistical tests, differences were considered as significant when $P < 0.05$. Data are presented as means ± s.d. Statistical analysis was performed using GraphPad Prism for Windows, version 4.0 (GraphPad Software, Inc., La Jolla, CA, USA).

RESULTS

Newly Formed Vasculature Is Surrounded by Proliferating Pericytes in the Ischemic Hemisphere at 3 Weeks of Reperfusion

RECA1-positive vessels were seen within the ischemic hemisphere at 24 hours, 48 hours, 7 days, and 3 weeks (Supplementary Figure 1). Colocalization of TUNEL, an indicator of cell death, and RECA1 was observed only at 48 hours. The number of blood vessels in ischemic hemispheres decreased from 24 hours to 7 days and increased at 3 weeks, and brain swelling was present at 24 and 48 hours (Figure 1A). By 3 weeks, increased density of vessels was seen within the peri-infarct areas (Figure 1B). Confocal microscopy showed that the vascular endothelial cells contained K₆₇ in the nuclei in the peri-infarct area, suggesting formation of new vessels (Figure 1C).¹⁵

The transmembrane proteoglycan, NG2, identifies pericytes in angiogenic microvasculature.¹⁶ Colabeling with NG2 and RECA1 showed low NG2 signal in sham-operated and contralateral hemispheres at 3 weeks after stroke. However, NG2-positive pericytes were seen around vessels identified by RECA1 in the peri-infarct areas (Figure 2A). Further confirmation that the NG2-positive cells were pericytes was obtained from confocal images that showed colocalization of NG2 with PDGFR- β (Figure 2B), an established early marker of activated pericytes. K₆₇ was expressed by pericytes in highly vascularized structures (Supplementary Figure 2A). The results confirmed the activated/angiogenic state of pericytes and substantiated their involvement in early angiogenesis.¹⁶

VEGF is a critical regulator of angiogenesis and barrierogenesis.¹⁷ At 3 weeks, there was increased expression of VEGF-A, an isoform of VEGF associated with angiogenesis, in the ischemic hemisphere compared with sham-operated and nonischemic ones (Supplementary Figure 2B). Adjacent to peri-infarct regions, VEGF-A colocalized with GFAP-positive astrocytes (Figure 2C). Within the peri-infarct regions, pericytes of microvessels expressed VEGF, while some pericytes expressing VEGF-A are to form mural cells of vessels (Figure 2C), as in embryogenesis.¹⁸

Functional Vasculature Remodeling in Peri-Infarct Regions

To determine functional neurovascular remodeling at 3 weeks after stroke, we used MRI¹⁹ and immunohistochemical analysis (Figure 3A). T2-weighted images and apparent diffusion coefficient (ADC) maps show greater hyperintensity in core infarcted areas than in peri-infarct regions. Dynamic contrast-enhanced MRI showed increased BBB transfer rate (K_i) and plasma volume (V_p) in the peri-infarct areas, while neither K_i nor V_p signal was seen in core infarct regions. To determine blood flow in these new vessels, cerebral blood flow perfusion was measured using ASL. Arterial spin labeling maps showed very low perfusion in the infarct core with hyperperfusion in the peri-infarct (mean ± s.e.: 127.2 ± 30.87 mL/100 g min, $n = 8$) compared with the contralateral hemisphere and intact areas (mean ± s.e.: 50.06 ± 7.433 mL/100 g min, $n = 8$) in the ischemic hemisphere ($P = 0.0291$). RECA1 immunostaining shows increased density of new vessels in peri-infarct areas, which corresponds to the regions with an elevated BBB transfer rate, plasma volume, and arterial blood perfusion. The H&E staining shows that red blood cells were located inside of microvessel-like structures. Intravenous injection of Evans blue showed fluorescence within vessels (Supplementary Figure 3A) along with Evans blue extravasation in the peri-infarct areas with vascular remodeling (Supplementary Figures 3B and C). These data suggested that some blood flow occurred in the new vessels, but permeability was increased at 3 weeks after stroke.

Tight Junction Proteins Expression in Newly Formed Vessels and Surrounding Astrocytes and Pericytes

From 24 hours to 7 days of reperfusion, occludin expression was rarely associated with RECA1-positive vessels in the ischemic hemispheres (Supplementary Figure 4A) and claudin-5 was undetectable (data not shown). By 3 weeks, we observed increased expression of occludin in cells surrounding vessels. The cells expressing occludin were GFAP-positive astrocytes that mostly bordered the peri-infarct areas (Supplementary Figure 4B) and were seen as early as 3 days after stroke (data not shown), while the cells that expressed occludin are neuron-like cells at 24 hours (Supplementary Figure 4C). Using triple-immunofluorescent staining and confocal microscopy, we found that the end-feet of astrocytes expressing occludin closely encapsulated endothelial cells (Figure 3B). Both astrocytes and vascular pericytes expressed ZO-1, another TJP associated with BBB permeability (Figure 3C). However, few endothelial cells colocalized with occludin or ZO-1 (Figures 3B and 3C), suggesting that astrocytes and pericytes are the major sources for these two TJPs during neurovascular remodeling. Unlike ZO-1, little occludin staining was seen surrounding the newly formed vessels within the peri-infarct areas. Colocalization of occludin and ZO-1 with RECA1 was seen in main vessels in nonischemic hemispheres, where occludin was also expressed by astrocyte-like cells (Supplementary Figure 5A and B). We observed a renewed expression of claudin-5 directly expressed by endothelial cells (CD31) in the peri-infarct regions at 3 weeks (Figure 3D). The claudin-5 in the endothelial cells had linear appearance, which is typical of TJPs in normal BBB.⁹

Matrix Metalloproteinase-2 and -3 Expressed by Vascular-Associated Astrocytes and Pericytes Are Involved in Neurovascular Remodeling

MMP-2 was expressed by astrocytes around the margin of infarcted areas (Figure 4A; Supplementary Figure 6A). Astrocyte end-feet, expressing MMP-2, contacted vessels inside peri-infarct regions. Strong MMP-3 immunostaining was seen closely along with vessels (Supplementary Figure 6B), but the double staining of MMP-3 and RECA1 showed MMP-3 was separated from the endothelial cells in peri-infarct areas (Figure 4B). Confocal three-dimensional (3D) and Z-stack images confirmed that the cells expressing MMP-3 were PDGFR- β - and NG2-positive pericytes

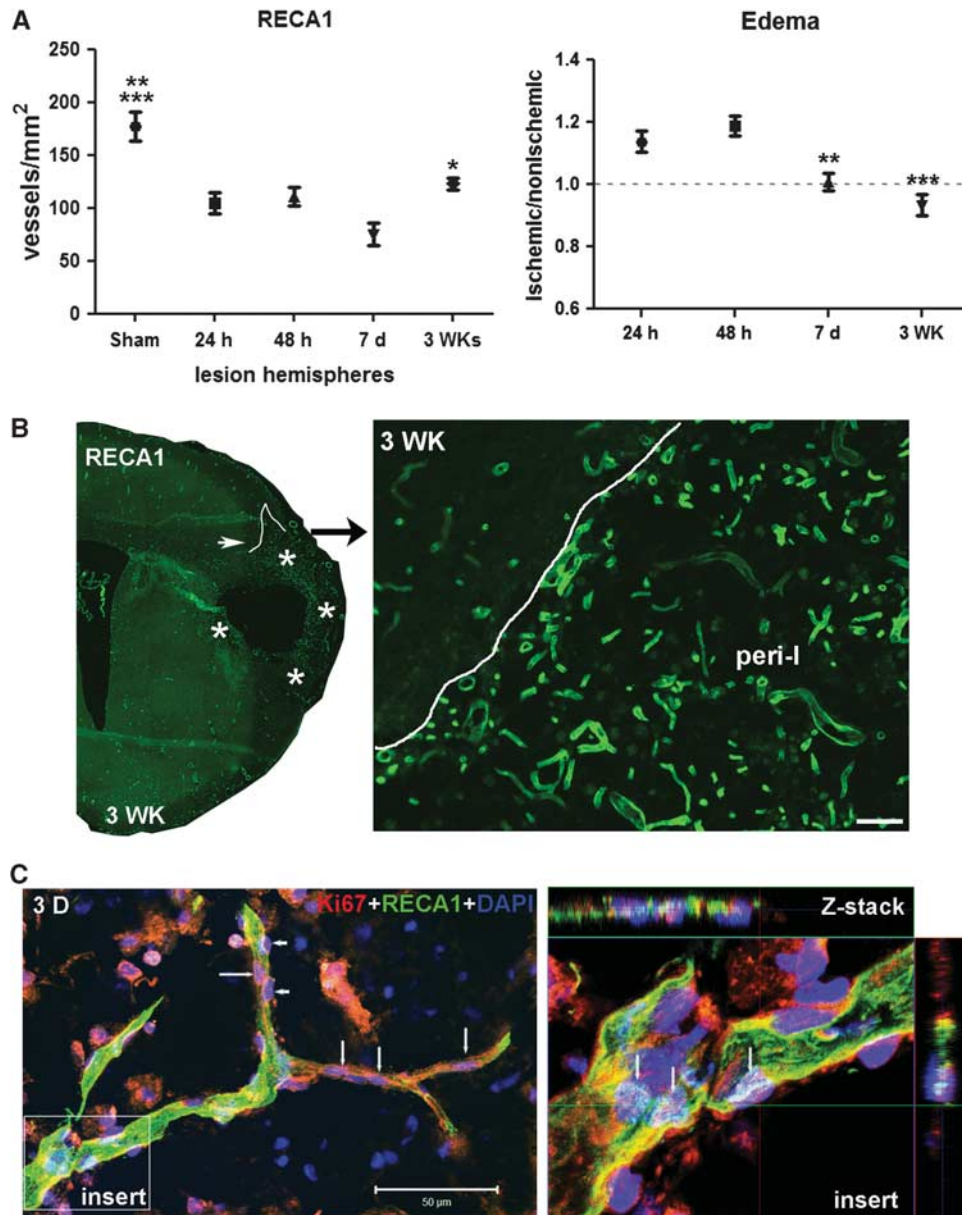


Figure 1. Increased number of newly formed vessels in ischemic hemispheres at 3 weeks of reperfusion. **(A)** Graph showing number of RECA1 staining microvessels in sham-operated and ischemic hemispheres. Focal ischemic stroke with reperfusion injury resulted in loss of RECA1-positive microvessels in ischemic hemispheres at 24 and 48 hours and 7 days. At 3 weeks after stroke, the number of RECA1-positive microvessels was increased compared with that at 7 days. $*P < 0.05$ vs. 7 days, $**P < 0.01$ vs. 48 hours and 3WK; $***P < 0.001$ vs. 24 hours and 7 days, $n = 6$ per group. The edema in ischemic hemispheres at 24 hours, 48 hours, 7 days, and 3 weeks of reperfusion compared with nonischemic hemispheres expressed as edema index. $**P < 0.01$, $***P < 0.001$ vs. 24 and 48 hours, respectively, $n = 6$ per group. The number of vessels was normalized for edema. **(B)** Immunohistochemistry of RECA1, a marker of endothelial cells, represents microvessels in peri-infarct area in ischemic hemisphere with reperfusion of 3 weeks (3WK). Lines outline the border of lesion areas. Stars indicate the peri-infarct area. Right panel shows the peri-infarct (peri-I) area in higher magnification. A higher density of microvessels was seen in the peri-infarct area. Scale bar = 50 μm . **(C)** Three-dimensional (3D) confocal microscopy shows that RECA1-positive vessel (green) contains nuclei expressing Ki67 (red, arrows), a marker of cell proliferation, in peri-infarct area at 3 weeks after stroke. Arrowheads show pericyte-like cells expressing Ki67. 4'-6-diamidino-2-phenylindole (DAPI) (blue) was used to stain nuclei. Z-stack confocal micrograph (insert) shows colocalization of Ki67 with DAPI in vascular endothelial cells (arrows). Scale bar = 50 μm .

surrounding the newly formed vessels (Figures 4C and D). Very low signal of MMP-9 was detectable at this time point (Supplementary Figure 6C). Furthermore, little colabeling of MMP-3 with OX-42-positive microglia/macrophages, GFAP-positive astrocytes, and NeuN-positive neurons showed that neither of these cell types were a significant source of MMP-3 (Supplementary Figure 7).

Early Inhibition of Matrix Metalloproteinase Activation Facilitates Angiogenesis and Tight Junction Protein Remodeling in Ischemic Hemispheres

At 3 weeks of reperfusion, the number of vessels in the rats treated with a single dose of GM6001 was significantly higher than that in vehicle-treated animals (Figure 5A). The increased level of VEGF-A seen in the ischemic hemispheres was augmented by

GM6001 treatment (Figure 5B). VEGF-A protein was also detected in the sham-operated hemisphere (Figure 5B; Supplementary Figure 2C), which may reflect the development of high blood pressure, altered vessel morphology, and growth factor expression in spontaneously hypertensive rats. Activin receptor-like kinases (ALK)1 and (ALK) 5 are transforming growth factor- β type I membrane receptors in brain microvessels and are important in angiogenesis. The ALK1 pathway leads to endothelial activation characterized by cellular proliferation and increased BBB permeability, while the ALK5-mediated signaling leads to impaired vascular proliferation and decreased BBB permeability.²⁰ The

levels of ALK1 and ALK5 in ischemic areas were significantly increased and decreased, respectively, compared with sham-operated rats. Treatment with GM6001 changed ALK1 and ALK5 protein levels (Figure 5C). These results suggest that early inhibition of MMP activity enhanced angiogenesis at 3 weeks of reperfusion.

Since we observed expression of TJPs and MMPs in vascular cells during recovery, we studied the impact of the early MMP inhibition on level of TJPs and MMPs at 3 weeks of reperfusion (Figure 6). As expected, ZO-1 was increased in the ischemic hemispheres and MMP inhibition significantly enhanced the level

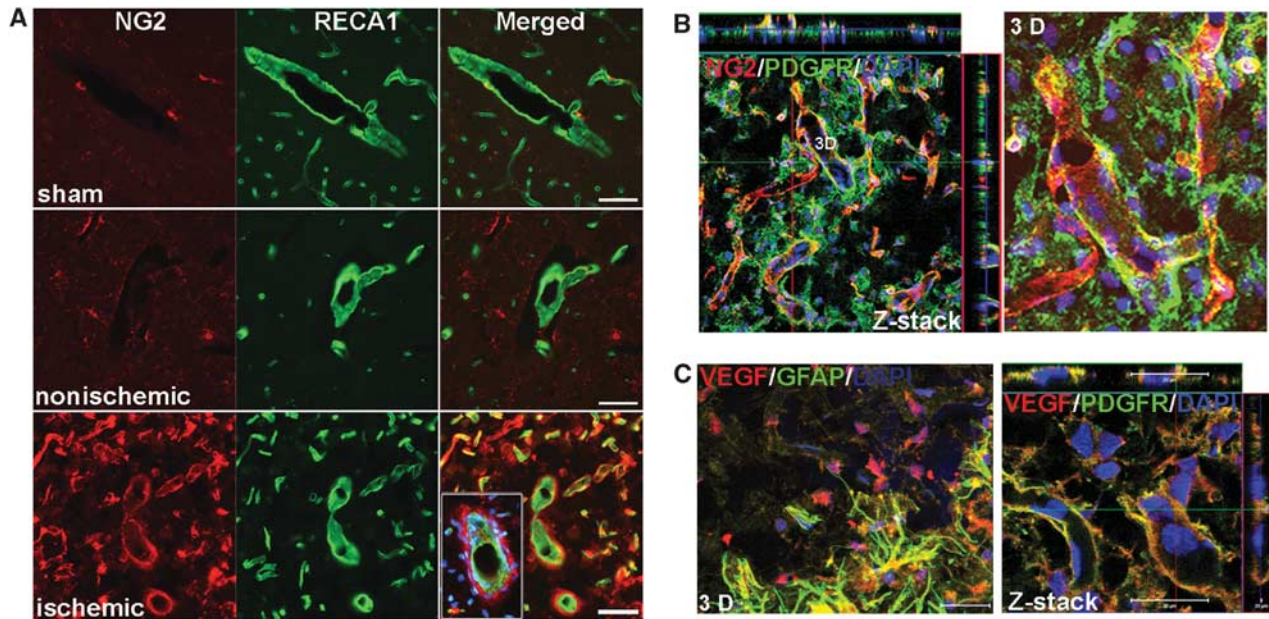
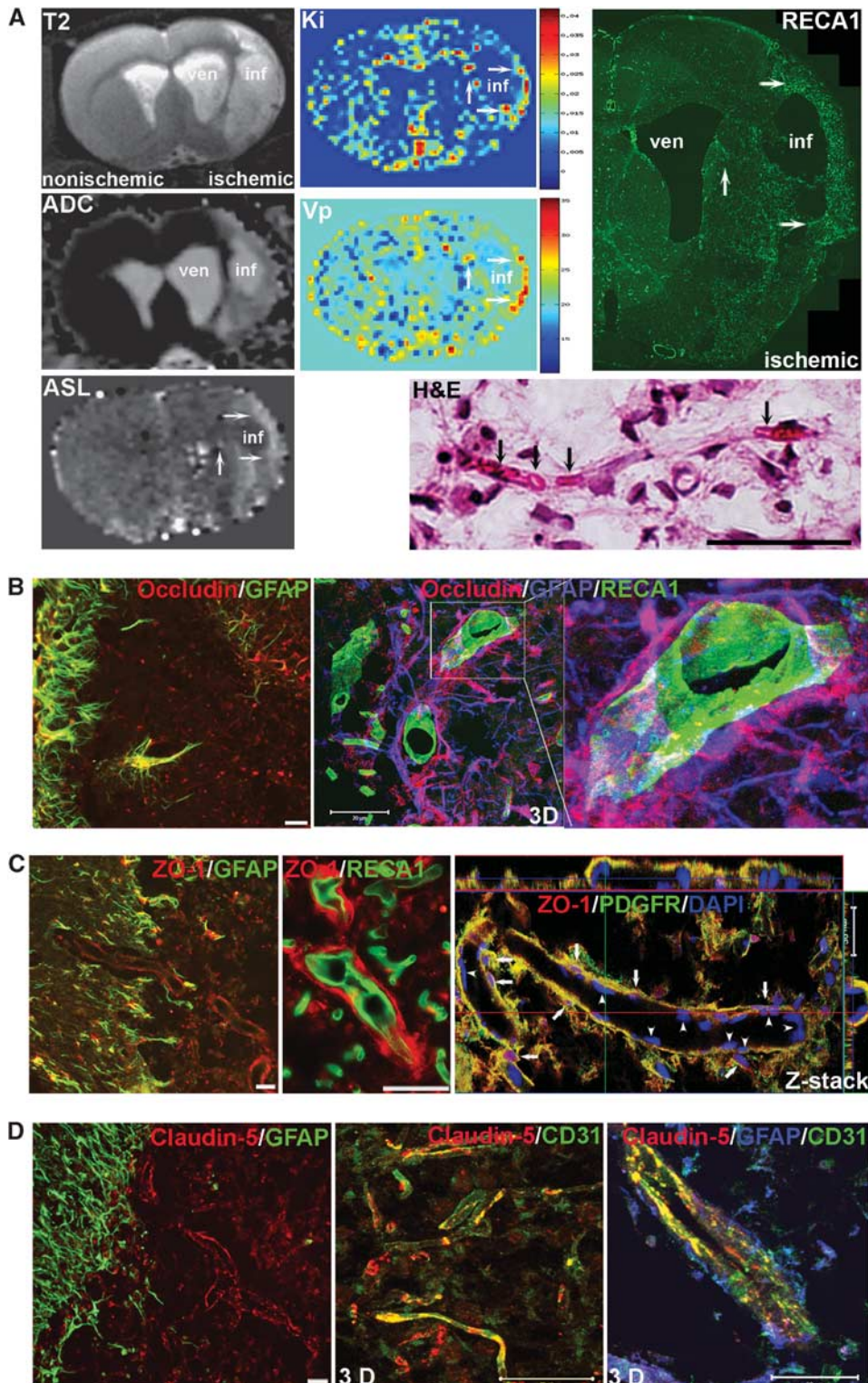


Figure 2. Angiogenesis is associated with proliferating vascular pericytes in peri-infarct area at 3 weeks of reperfusion. (A) Micrographs show double-labeled NG2 and RECA1 in sham-operated, nonischemic, and ischemic hemispheres. NG2 antibody was used to identify immature pericytes, which indicate newly formed vessels. Increased immunostaining of NG2 was seen in the peri-infarct region, which specifically stained only the pericyte layer that was tightly apposed to the RECA1-positive microvessels. The insert represents a vessel cut transversely with NG2-positive pericytes surrounding it. 4'-6-diamidino-2-phenylindole (DAPI) (blue) was used to stain nuclei. Scale bars = 50 μ m. (B) Z-stack and three-dimensional (3D) confocal micrographs show colocalization of NG2 (red) with PDGFR- β (PDGFR, green, a marker of pericytes) in vascular structures in peri-infarct region. In the Z-stack image, the inner layer of the vascular structures labeled with DAPI, indicating endothelial cells show no colocalization with NG2 and PDGFR- β . (C) Double immunostaining of VEGF-A (red) with GFAP (green) and PDGFR- β (green). 3D micrograph shows increased VEGF-A colocalized with astrocytes (GFAP) around the peri-infarct region. Within the peri-infarct region, Z-stack confocal micrograph indicates the vascular pericytes (PDGFR) expressing VEGF-A. DAPI was used to stain nuclei. Scale bars = 20 or 50 μ m.

Figure 3. Blood flow, blood-brain barrier (BBB) permeability, and expression of tight junction proteins (TJPs) in the new vessels within peri-infarct regions 3 weeks of reperfusion. (A) Hyperintensive areas in the anatomic T2 image and apparent diffusion coefficient (ADC) map show the lesion extent and tissue ischemia. ven: Ventricle; inf: Core infarct area. Color-coded permeability coefficient maps reconstructed from dynamic contrast-enhanced magnetic resonance imaging (MRI) data show the regions of high (red) and low (blue) permeability. Parametric image K_i map represents BBB transfer rate. Parametric image V_p map represents plasma volume. Elevated values of K_i and V_p are located in the vicinity of core infarct area (arrows). There are no signals of K_i and V_p in core infarct area. The color scales used for the permeability and plasma volume signal intensity. Arterial spin labeling (ASL) map shows higher cerebral blood flow (CBF) in peri-infarct areas (arrows). RECA1 immunostaining shows increased density of new vessels in peri-infarct area (arrows), corresponding to the elevated BBB transfer rate, plasma volume and blood perfusion (arrows). Hematoxylin and Eosin (H&E) staining shows red blood cells located inside of the new microvessels (arrows). (B) Left panel: double immunostaining of occludin (red) with astrocytes (GFAP, green) shows that occludin was colocalized with reactive astrocytes adjacent to or within the peri-infarct region. Middle and right panels: triple immunostaining of occludin (red) with astrocytes (blue) and endothelial cells (green). The 3D confocal images show that astrocytes expressing occludin (shown in purple when colocalized) with end-feet closely surrounding vessels. (C) Double immunostaining of zonula occludens-1 (ZO-1) with astrocytes, endothelial cells, and pericytes (PDGFR), respectively. ZO-1 colocalized with reactive astrocytes (GFAP) but not with endothelial cells (RECA1). Z-stack confocal image shows pericytes (green) surrounding vessels express ZO-1 (arrows). Arrowheads indicate 4'-6-diamidino-2-phenylindole (DAPI)-stained endothelium. (D) Double immunostaining shows no colocalization (left panel) between astrocytes (green) and claudin-5 (red). The 3D confocal image (middle panel) shows that claudin-5 was colocalized with endothelial cells (CD31, green) of microvessels within the peri-infarct region. Confocal image (right panel) of triple immunostaining shows that astrocytes (blue) surround a vessel with claudin-5 in endothelial cells (green). Scale bars = 20 or 50 μ m.

of ZO-1 (Figure 6A). Occludin could have many isoforms and the oligomeric assemblies of occludin are alternately under conditions of hypoxia and reoxygenation stress.^{21,22} At 3 weeks, we detected five bands of occludin from ~20 to 65 kDa in ischemic rat brains. Significantly increased occludin levels (all bands) were seen in ischemic hemisphere compared with sham animals, while treatment with GM6001 promoted the level of occludin (Supplementary Figure 8A). Occludin was expressed as 65 kDa

(β -band) and 63 kDa (α -band) bands, which suggests the presence of phosphorylated and nonphosphorylated forms, respectively.²³ There was a significant decrease in occludin levels in both ischemic and nonischemic hemispheres of vehicle-treated animals. Treatment with GM6001 promoted the expression of occludin compared with vehicle-treated rats. We observed that ischemia induced an integral change in occludin between the β - and α -bands. After ischemia, the major band of occludin shifted



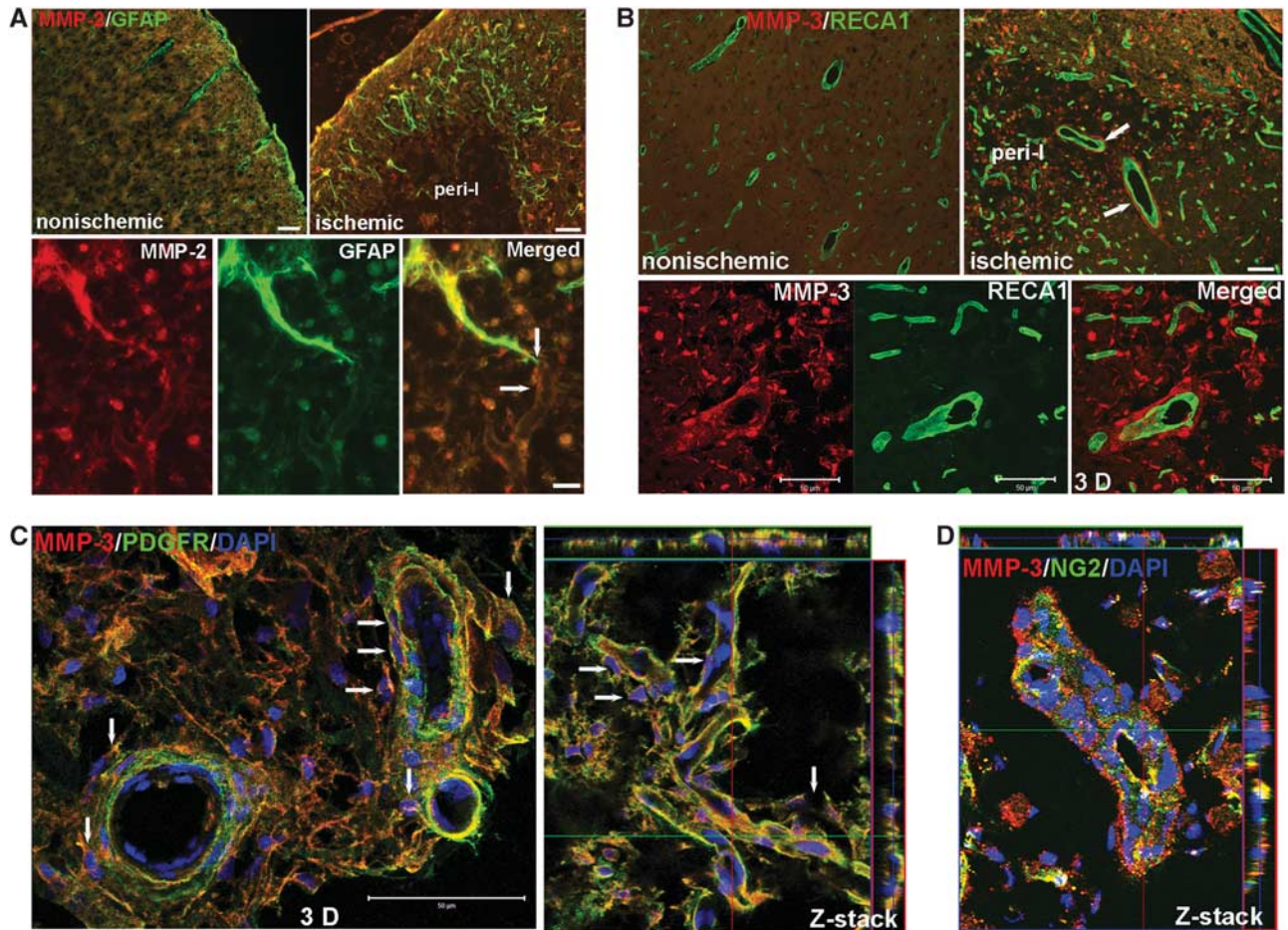


Figure 4. Increased expression of matrix metalloproteinase (MMP)-2 and MMP-3 in astrocytes and vascular pericytes in peri-infarct areas at 3 weeks of reperfusion. **(A)** Micrographs show the location of MMP-2 (red) in peri-infarct cortex. Increased expression of MMP-2 was seen in reactive astrocytes (green) around the border of lesion areas compared with nonischemic cortex. The endfeet of astrocytes expressing MMP-2 connect to vessels within peri-infarct areas (bottom panel, arrows). **(B)** Micrographs showing the location of MMP-3 (red) in peri-infarct cortex. Increased expression of MMP-3 was seen in peri-infarct cortex compared with nonischemic cortex. Large vessels (RECA1, green) are surrounded by cells expressing MMP-3 (arrows) but are not colocalized with MMP-3. Three-dimensional (3D) confocal microscopy analysis presents the spatial distribution of MMP-3 around vessels. **(C)** Confocal microscopy shows the cells that express MMP-3 around vessels are PDGFR- β -positive pericytes (green). 3D image showed pericytes expressing MMP-3 closely surrounded main vessels (arrows). Z-stack image shows colocalization of PDGFR- β with MMP-3 around microvessels with some pericytes expressing MMP-3 in contacting these vessels (arrows). 4'-6-diamidino-2-phenylindole (DAPI) (blue) was used to stain nuclei. **(D)** Z-stack confocal micrograph shows colocalization of NG2 and MMP-3. Scale bars = 20 or 50 μ m.

from the β -band to the α -band compared with sham-operated rats. Importantly, treatment with GM6001 enhanced the β -band intensity, which made the ratio of the β -band to α -band similar to that of sham-operated rats. We found a significant increase in claudin-5, including 22 and 17 kDa bands, in ischemic hemispheres by 3 weeks. The increase was less significant in GM6001-treated rats. However, a cleaved band at 17 kDa was seen in the vehicle-treated animals, but not in the GM6001-treated animals. One of the possibilities is that the presence of the 17-kDa band indicated that the claudin-5 in the new vessels is being incorporated. Taken together, these results suggest that early inhibition of MMP activity can enhance TJP formation.

Pro- and active MMP-2 (68 and 62 kDa, respectively)⁸ and MMP-3 (57 and 45 kDa, respectively) significantly increased in both vehicle and GM6001-treated rats at 3 weeks of reperfusion, but higher levels were observed in GM6001-treated rats (Figure 6B). Furthermore, western blots of MMP-2 show that MMP inhibition significantly increased expression of pro-MMP-2 (68 kDa) in ischemic hemispheres, which, like occludin, approached the intensity of MMP-2 seen in sham-operated rats.

Early Inhibition of Matrix Metalloproteinase Activation Reduces Brain Tissue Loss During Recovery

Treatment with GM6001 significantly reduced infarct size at 24 hours (Supplementary Figures 8A and B) and tissue loss at 3 weeks of reperfusion (Figure 7A). The MRI confirmed the effect of GM6001 treatment in rats with an extended reperfusion at 4 weeks. Anatomic T2 MRI illustrated that treatment with GM6001 significantly reduced the size of lesion areas in ischemic hemispheres (Figure 7B). Increase in the ADC value was found in the ischemic hemispheres, suggesting increased diffusivity in the regions of tissue loss. Significantly lower ADC values in the GM6001-treated ischemic hemisphere were observed compared with the vehicle-treated brain. This was seen postmortem in the cavitation of infarcted cortex at 4 weeks, which was markedly attenuated by GM6001 treatment (Figure 7C).

DISCUSSION

We show that vascular-associated pericytes and astrocytes are the major source of TJPs, MMPs, and VEGF for newly formed

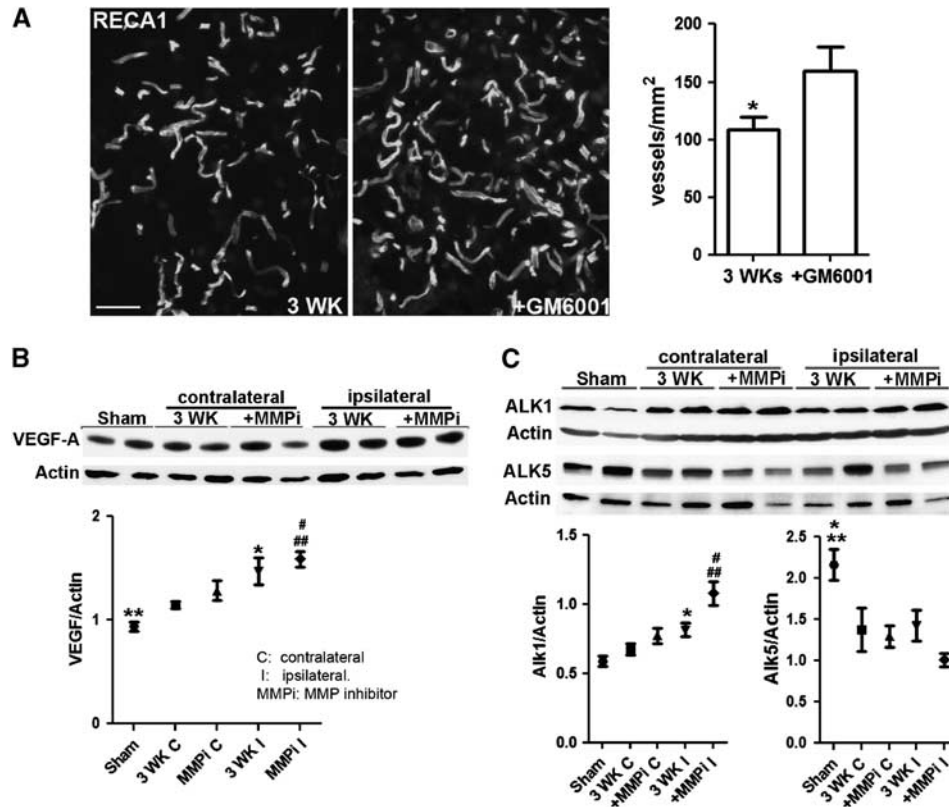


Figure 5. Promotion of angiogenesis in ischemic hemisphere by early inhibition of matrix metalloproteinases (MMPs). **(A)** Micrographs representing RECA1 staining microvessels in peri-infarct areas in rat brains with or without GM6001 treatment at 3 weeks of reperfusion. Significantly higher number of microvessels were detected in GM6001-treated rat compared with vehicle, $*P < 0.05$, $n = 6$ per group. **(B)** Western blot analysis showing an increase in the VEGF-A level in ischemic rat brain tissues. $**P < 0.01$ vs. 3 WK I and MMP inhibitor (MMPi) I; $*P < 0.05$ vs. 3 WK C; $\#P < 0.01$ vs. 3 WK C. Higher level of VEGF-A was detected in GM6001-treated ischemic hemispheres compared with vehicle-treated one, but not statistically significant. $n = 9$ per group. **(C)** Western blot analysis showing changes in levels of activin receptor-like kinase (ALK) 1 and 5 in rat brain tissues. ALK1 level increased in ischemic rat brains at 3 weeks of reperfusion and treatment with MMPi significantly facilitated the expression of ALK1. $*P < 0.01$ vs. sham and 3 WK C; $\#P < 0.01$ vs. MMPi C and 3 WK I; $\#\#\#P < 0.001$ vs. sham and 3 WK C. The ALK5 level decreased at 3 weeks of reperfusion. $*P < 0.05$ vs. 3 WK C, 3 WK I, and MMPi C; $**P < 0.01$ vs. MMPi I. Treatment with MMPi reduced ALK5 expression compared with vehicle-treated group (3 WK), $P = 0.055$. $n = 6$ in sham group, 9 in vehicle and GM6001-treated groups.

vessels in peri-infarct areas at 3 weeks of reperfusion. We found an association between MMPs and formation of TJPs in brain vessels during angiogenesis. We propose that these MMPs contribute to functional remodeling of the BBB during recovery after stroke, and that short-term early inhibition of MMPs promotes these processes, facilitating recovery.

Angiogenesis provides critical neurovascular substrates for remodeling after stroke by generating new vessels necessary for neurogenesis and synaptogenesis.^{1,24–26} Factors released by endothelial cells *in vitro* trigger neural stem cell proliferation and angiogenesis, contributing to functional recovery.²⁷ We found that some vessels remain in the lesion areas up to 7 days after reperfusion, which could provide the cellular basis to trigger angiogenesis.^{1,17} Other studies showed that endothelial cells surrounding the infarcted area start to proliferate as early as 12 to 24 hours, leading to increased vessels in the peri-infarcted region 3 days after ischemic injury.^{28,29} We found pericytes surrounded the increased number of regrowing endothelial cells seen in the ischemic hemispheres at 3 weeks of reperfusion. These vascular-associated pericytes are NG2 and K₆₇ positive, suggesting that they are newly formed and contribute to new vessel proliferation in the peri-infarct regions.^{16,30} Pericytes have a key role in the development of cerebral vasculature and control key neurovascular functions and neuronal phenotype in the adult brain and during brain aging.^{17,31–33} Our results show that

proliferating vascular pericytes participate in the neo-vascularization of peri-infarct areas after stroke by expressing TJPs, VEGF, and MMP-3. It is known that the NG2 proteoglycan is expressed by microvascular pericytes in newly formed blood vessels. Along with its ability of revealing the activated/angiogenic state of microvessels, the pericyte-derived NG2 is an important factor in promoting endothelial cell migration and morphogenesis during the early stages of neo-vascularization.³⁴ Pathologic angiogenesis can be reduced by targeting pericytes via the NG2 proteoglycan. In NG2 knock-out mice, proliferation of both pericytes and endothelial cells in retina in response to hypoxia is significantly reduced.³⁰ There are several possible mechanisms by which NG2 regulates angiogenesis; NG2 has been shown to bind directly to basic fibroblast growth factor and platelet-derived growth factor AA (PDGF-AA), and may enhance interaction of these growth factors with cell surface receptors.¹⁶ In the present study, we showed an overexpression of NG2 in vascular-associated pericytes at 3 weeks, which is spatiotemporally expressed with MMPs, VEGF, and TJPs. Further studies will be needed to investigate whether NG2 interacts with these proteins and the impact of these interactions on the BBB remodeling after stroke.

At 3 weeks in spite of the presence of TJPs in pericytes, astrocytes, and endothelial cells, we observed BBB leakage in the peri-infarct regions where new vessels are located, indicating that

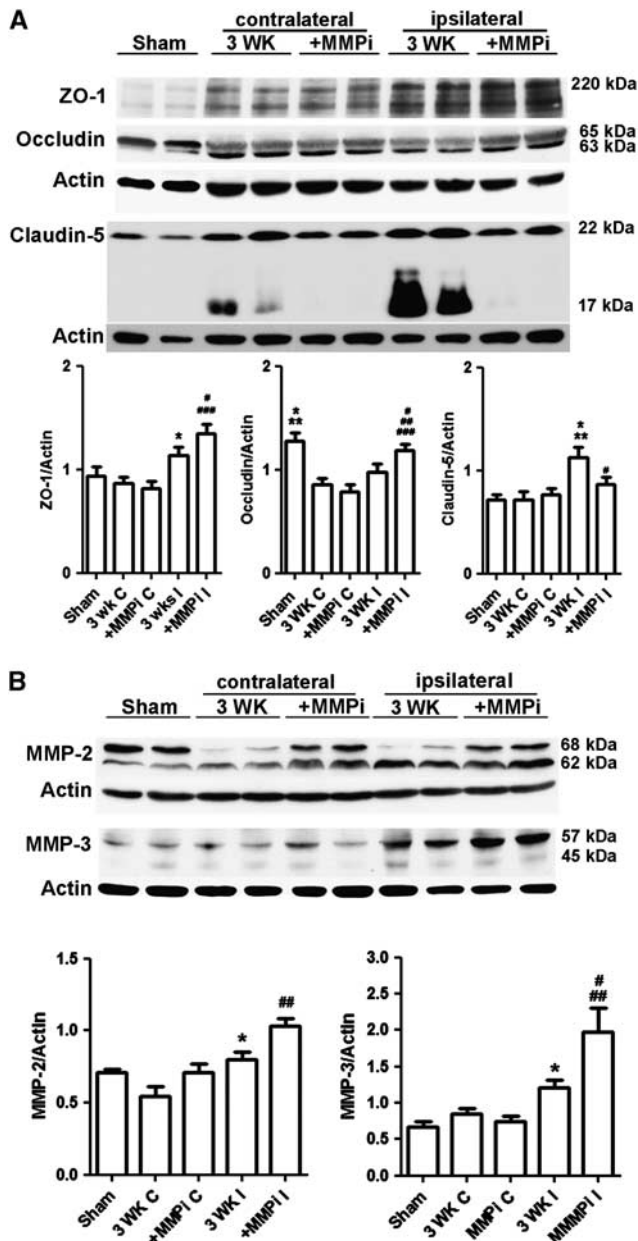


Figure 6. Early inhibition of matrix metalloproteinases (MMPs) enhances expressions of tight junction proteins (TJPs) and MMPs at 3 weeks of reperfusion. **(A)** Western blot analysis of TJPs in sham-operated, nonischemic, and ischemic hemispheres. Zonula occludens-1 (ZO-1) (includes bands of 220 and 210 kDa); * $P < 0.05$ vs. 3 WK C and MMPi C; # $P < 0.05$ vs. sham; ### $P < 0.001$ vs. 3 WK C and MMPi C. Occludin (includes bands of 65 and 63 kDa); * $P < 0.05$ vs. 3 WK I; ** $P < 0.01$ vs. 3 WK C and MMPi C; # $P < 0.05$ vs. 3 WK I; ### $P < 0.01$ vs. 3 WK C; ### $P < 0.001$ vs. MMPi C. Claudin-5 (includes bands of 22 and 17 kDa); * $P < 0.05$ vs. sham; ** $P < 0.01$ vs. 3 WK C and MMPi C; # $P < 0.05$ vs. 3 WK I. **(B)** Western blot analysis of MMP-2 and -3 in sham-operated, nonischemic, and ischemic hemispheres. MMP-2 includes pro-MMP-2 (68 kDa) and active MMP-2 (62 kDa). * $P < 0.05$ vs. 3 WK C. ### $P < 0.01$ vs. sham, 3 WK C, MMPi C, and MMPi I. MMP-3 includes pro-MMP-3 (57 kDa) and active MMP-3 (45 kDa). * $P < 0.05$ vs. sham and 3 WK C; # $P < 0.05$ vs. sham; ### $P < 0.01$ vs. 3 WK C and MMPi C. Treatment with MMPi I increased MMP-3 expression compared with vehicle-treated group (3 WK I), $P = 0.051$. $n = 6$ in sham group, 9 in vehicle- and GM6001-treated groups.

while new vessels may have blood flow, barrier properties are not yet fully developed. We observed occludin, claudin-5, and ZO-1 in NVU cells in the peri-infarct regions at 3 weeks after stroke. Only claudin-5, which disappeared in BBB from 24 hours to 7 days after stroke, reappeared in the newly formed endothelial cells. The other major TJPs, occludin and ZO-1, were absent from endothelial cells, but were prominent in the GFAP-positive reactive astrocytes, which extended processes to closely encapsulate nearby endothelial cells. A striking collection of NG2-positive pericytes entirely surrounded vascular endothelial cells and produced ZO-1. Thus, the TJPs normally seen within endothelial cells where they form the first barrier to blood-borne substances were redistributed to pericytes and astrocytes, which failed to provide a barrier to Evans blue or Gadolinium, suggesting that the TJPs in perivascular cells do not form a functional barrier. Whether the TJPs eventually move into the endothelial cells or are made *de novo* will need further study.

Vascular-associated astrocytes and pericytes expressed VEGF, a major stimulator of developmental and disease-related angiogenesis. During development, pericytes release angiopoietin-1, which induces the formation of tight junctions by binding to the Tie-2 receptor localized on endothelial cells.¹ The VEGF in astrocytes and pericytes may provide a microenvironment that favors this process during neurovascular remodeling.

Pericytes and astrocytes, which contain TJPs and VEGF, expressed the MMP-2 and -3 in the peri-infarct areas at 3 weeks after stroke. While MMPs are damaging in acute brain injury, they are necessary for later angiogenesis and neurogenesis.¹⁰ When treatment with MMP inhibitors is given over several days, they induce hemorrhage, interfere with neuroplasticity, and slow recovery. In angiogenesis, loss of vascular integrity and degradation of the extracellular matrix are crucial initiating steps. Matrix metalloproteinases degrade the extracellular matrix preparing the stage for growth factors and guidance molecules, which explains the paradoxical finding that MMP inhibition has dual effects. Most likely this function is performed by the MMP-3 expressed by NG2-positive pericytes that are located next to new vessels, where they can degrade extracellular matrix and facilitate vessel migration into the infarcted tissues. This endothelial migration is aided by growth factors, including VEGF.³²

An important finding of our study was that a single dose of an MMP inhibitor administered early in the stroke benefits neurovascular remodeling during the recovery phase. We have showed the neuroprotective role of early MMP inhibition on ischemia-induced BBB disruption, and on the neuronal apoptotic death induced by intranuclear MMP activity.^{8,9,35} This neuroprotective role of early MMP inhibition on BBB reduced its permeability, which may attenuate the secondary injury, such as entrance of neurotoxic blood compounds, infiltration of inflammatory cells, and systematic MMPs, especially neutrophil-derived MMP-9 into the brain soon after reperfusion.^{36,37} We hypothesized promoting survival of blood vessels and brain cells from ischemic injury and BBB integrity will provide the cellular and molecular basis to promote later angiogenesis. With both histologic and MRI techniques, we found reduced tissue loss in GM6001-treated animals during recovery after stroke. Treatment with GM6001 showed a number of beneficial effects, including greater numbers of newly formed vessels, increased levels of VEGF protein, TJP formation with proliferation of endothelial cells, increased ALK1 expression, and reduced ALK5 expression.²⁰ Treatment with GM6001 enhanced the level of the phosphorylated form of occludin (65 kDa), which is the tetraspan integral membrane protein that localizes endothelial tight junctions, and contributes to tight junction stabilization and optimal barrier function. Phosphorylation is a possible mechanism that controls occludin localization and function.³⁸ Occludin phosphorylation and subsequent ubiquitination are necessary for VEGF-induced TJP

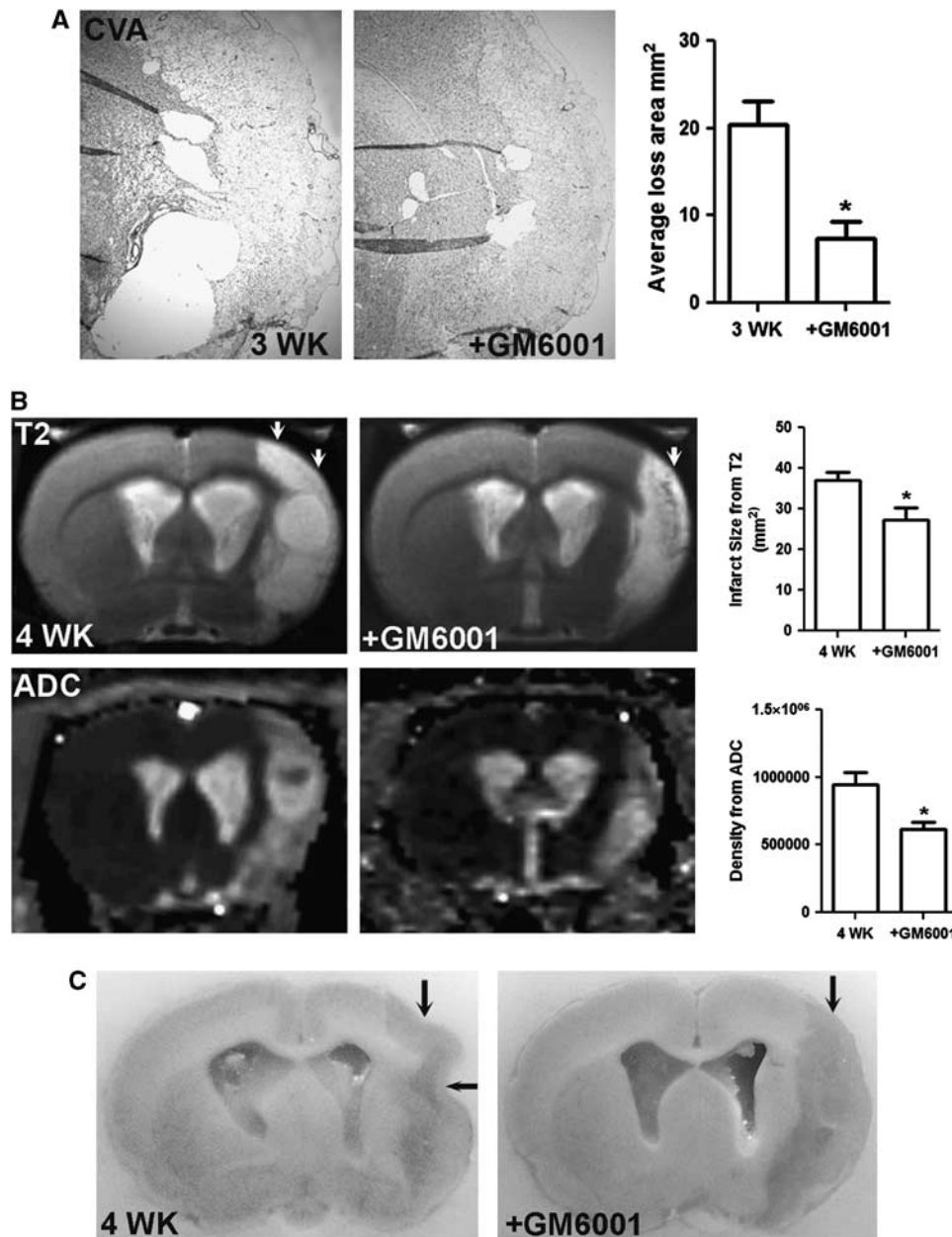


Figure 7. Matrix metalloproteinase (MMP) inhibition improves outcomes by reducing brain tissue loss during recovery. **(A)** Cresyl violet acetate (CVA) staining represents tissue loss (blank areas) in ischemic hemispheres with or without GM6001 treatment at 3 weeks of reperfusion. Bar graphs show that treatment with GM6001 significantly reduced tissue loss. $*P < 0.05$, $n = 6$ per group. **(B)** Anatomic T2 magnetic resonance (MR) images show the tissue lesion extent (arrows) in ischemic hemispheres with or without GM6001 treatment at 4 weeks of reperfusion. Treatment with GM6001 significantly reduced the lesion size. Apparent diffusion coefficient (ADC) maps reconstructed from raw diffusion-weighted image (DWI) data show lesion regions of increased ADC values (hyperintense regions) with the region of lower value on the GM6001-treated ischemic hemisphere. $*P < 0.01$, $n = 5$ for each group. **(C)** Perfused brains shown in **(B)**. After perfusion and fixation with 2% paraformaldehyde, the tissue loss in infarcted cortex in vehicle-treated brain was manifested as a collapse of the ischemic hemisphere (arrows). Reduced cavitation of infarcted cortex was seen in rats treated with GM6001.

trafficking and endothelial permeability.³⁹ Importantly, the expression of MMP-2 and -3 during the recovery stages was not impaired by the early single dose of an MMP inhibitor.

It is important to point out that the ischemia-induced increase in MMP-2 and -9 at 3 and 24 hours is expressed by reactive astrocytes and neurons within infarct areas, which were damaged and died after 24 to 48 hours, no change of MMP-3 mRNA transcription was detected at 3 hours of reperfusion.^{9,35} The astrocytes that expressed MMP-2 at 3 weeks are a new population surrounding peri-infarct regions that begin to appear after 3 days of reperfusion.^{10,40} Matrix metalloproteinase-9 is

upregulated in peri-infarct cortex at 7 to 14 days after stroke and is colocalized with markers of neurovascular remodeling. Treatment with MMP inhibitors at 7 days after stroke suppresses neurovascular remodeling, increases ischemic brain injury, and impairs functional recovery at 14 days.¹⁰ Our previous study showed the new population astrocytes expressed MMP-3 at 3 days after stroke,⁴⁰ while in the present study we found that the proliferating pericytes in the peri-infarct areas are the major source of MMP-3 at 3 weeks. These findings suggest that careful timing of delivery of MMP inhibitors after stroke might present a feasible therapeutic approach. Since these studies were

performed with the inhibitor given at the onset of ischemia, further studies are needed with the inhibitor given shortly after the stroke onset.

DISCLOSURE/CONFLICT OF INTEREST

The authors declare no conflict of interest.

AUTHOR CONTRIBUTIONS

YY conceived and designed the experiments and wrote the manuscript. YY, JFT, VMS, and TM performed biochemical and histologic studies and data analysis. EYE and YY performed the MCAO surgery. ST, YRY, and YY performed MRI scan and data analysis. JWH performed biochemical experiments. GAR provided scientific advice in the execution of the study and in writing the report.

REFERENCES

- Hermann DM, Zechariah A. Implications of vascular endothelial growth factor for postischemic neurovascular remodeling. *J Cereb Blood Flow Metab* 2009; **29**: 1620–1643.
- Arai K, Jin G, Navaratna D, Lo EH. Brain angiogenesis in developmental and pathological processes: neurovascular injury and angiogenic recovery after stroke. *FEBS J* 2009; **276**: 4644–4652.
- Krupinski J, Kaluza J, Kumar P, Kumar S, Wang JM. Some remarks on the growth-rate and angiogenesis of microvessels in ischemic stroke. Morphometric and immunocytochemical studies. *Patol Pol* 1993; **44**: 203–209.
- Zhu W, Fan Y, Hao Q, Shen F, Hashimoto T, Yang GY et al. Postischemic IGF-1 gene transfer promotes neurovascular regeneration after experimental stroke. *J Cereb Blood Flow Metab* 2009; **29**: 1528–1537.
- Shen F, Walker EJ, Jiang L, Degos V, Li J, Sun B et al. Coexpression of angiopoietin-1 with VEGF increases the structural integrity of the blood-brain barrier and reduces atrophy volume. *J Cereb Blood Flow Metab* 2011; **31**: 2343–2351.
- Dejonckheere E, Vandenbroucke RE, Libert C. Matrix metalloproteinases as drug targets in ischemia/reperfusion injury. *Drug Discov Today* 2011; **16**: 762–778.
- Gu Z, Cui J, Brown S, Fridman R, Mobashery S, Strongin AY et al. A highly specific inhibitor of matrix metalloproteinase-9 rescues laminin from proteolysis and neurons from apoptosis in transient focal cerebral ischemia. *J Neurosci* 2005; **25**: 6401–6408.
- Yang Y, Candelario-Jalil E, Thompson JF, Cuadrado E, Estrada EY, Rosell A et al. Increased intranuclear matrix metalloproteinase activity in neurons interferes with oxidative DNA repair in focal cerebral ischemia. *J Neurochem* 2010; **112**: 134–149.
- Yang Y, Estrada EY, Thompson JF, Liu W, Rosenberg GA. Matrix metalloproteinase-mediated disruption of tight junction proteins in cerebral vessels is reversed by synthetic matrix metalloproteinase inhibitor in focal ischemia in rat. *J Cereb Blood Flow Metab* 2007; **27**: 697–709.
- Zhao BQ, Wang S, Kim HY, Storrer H, Rosen BR, Mooney DJ et al. Role of matrix metalloproteinases in delayed cortical responses after stroke. *Nat Med* 2006; **12**: 441–445.
- Li C, Engstrom G, Hedblad B, Berglund G, Janzon L. Blood pressure control and risk of stroke: a population-based prospective cohort study. *Stroke* 2005; **36**: 725–730.
- Amantea D, Russo R, Gliozzi M, Fratto V, Berliocchi L, Bagetta G et al. Early upregulation of matrix metalloproteinases following reperfusion triggers neuroinflammatory mediators in brain ischemia in rat. *Int Rev Neurobiol* 2007; **82**: 149–169.
- Sood R, Yang Y, Taheri S, Candelario-Jalil E, Estrada EY, Walker EJ et al. Increased apparent diffusion coefficients on MRI linked with matrix metalloproteinases and edema in white matter after bilateral carotid artery occlusion in rats. *J Cereb Blood Flow Metab* 2009; **29**: 308–316.
- Taheri S, Sood R. Partial volume effect compensation for improved reliability of quantitative blood-brain barrier permeability. *Magn Reson Imaging* 2007; **25**: 613–625.
- Li L, Harms KM, Ventura PB, Lagace DC, Eisch AJ, Cunningham LA. Focal cerebral ischemia induces a multilineage cytogenic response from adult subventricular zone that is predominantly gliogenic. *Glia* 2010; **58**: 1610–1619.
- Virgintino D, Girolamo F, Errede M, Capobianco C, Robertson D, Stallcup WB et al. An intimate interplay between precocious, migrating pericytes and endothelial cells governs human fetal brain angiogenesis. *Angiogenesis* 2007; **10**: 35–45.
- Lee HS, Han J, Bai HJ, Kim KW. Brain angiogenesis in developmental and pathological processes: regulation, molecular and cellular communication at the neurovascular interface. *FEBS J* 2009; **276**: 4622–4635.
- Daneman R, Zhou L, Kebede AA, Barres BA. Pericytes are required for blood-brain barrier integrity during embryogenesis. *Nature* 2010; **468**: 562–566.
- Seevinck PR, Deddens LH, Dijkhuizen RM. Magnetic resonance imaging of brain angiogenesis after stroke. *Angiogenesis* 2010; **13**: 101–111.
- Ronaldson PT, Demarco KM, Sanchez-Covarrubias L, Solinsky CM, Davis TP. Transforming growth factor-beta signaling alters substrate permeability and tight junction protein expression at the blood-brain barrier during inflammatory pain. *J Cereb Blood Flow Metab* 2009; **29**: 1084–1098.
- Cummins PM. Occludin: one protein, many forms. *Mol Cell Biol* 2012; **32**: 242–250.
- McCaffrey G, Willis CL, Staats WD, Nametz N, Quigley CA, Hom S et al. Occludin oligomeric assemblies at tight junctions of the blood-brain barrier are altered by hypoxia and reoxygenation stress. *J Neurochem* 2009; **110**: 58–71.
- Witt KA, Mark KS, Hom S, Davis TP. Effects of hypoxia-reoxygenation on rat blood-brain barrier permeability and tight junctional protein expression. *Am J Physiol Heart Circ Physiol* 2003; **285**: H2820–H2831.
- Brea D, Sobrino T, Ramos-Cabrer P, Castillo J. Reorganization of the cerebral vasculature following ischaemia. *Rev Neurol* 2009; **49**: 645–654.
- Nakagomi N, Nakagomi T, Kubo S, Nakano-Doi A, Saino O, Takata M et al. Endothelial cells support survival, proliferation, and neuronal differentiation of transplanted adult ischemia-induced neural stem/progenitor cells after cerebral infarction. *Stem Cells* 2009; **27**: 2185–2195.
- Teng H, Zhang ZG, Wang L, Zhang RL, Zhang L, Morris D et al. Coupling of angiogenesis and neurogenesis in cultured endothelial cells and neural progenitor cells after stroke. *J Cereb Blood Flow Metab* 2008; **28**: 764–771.
- Shen Q, Goderie SK, Jin L, Karanth N, Sun Y, Abramova N et al. Endothelial cells stimulate self-renewal and expand neurogenesis of neural stem cells. *Science* 2004; **304**: 1338–1340.
- Beck H, Plate KH. Angiogenesis after cerebral ischemia. *Acta Neuropathol* 2009; **117**: 481–496.
- Hayashi T, Noshita N, Sugawara T, Chan PH. Temporal profile of angiogenesis and expression of related genes in the brain after ischemia. *J Cereb Blood Flow Metab* 2003; **23**: 166–180.
- Ozderem U, Stallcup WB. Pathological angiogenesis is reduced by targeting pericytes via the NG2 proteoglycan. *Angiogenesis* 2004; **7**: 269–276.
- Bell RD, Winkler EA, Sagare AP, Singh I, LaRue B, Deane R et al. Pericytes control key neurovascular functions and neuronal phenotype in the adult brain and during brain aging. *Neuron* 2010; **68**: 409–427.
- Dore-Duffy P, LaManna JC. Physiologic angiodynamics in the brain. *Antioxid Redox Signal* 2007; **9**: 1363–1371.
- Al Ahmad A, Taboada CB, Gassmann M, Ogunshola OO. Astrocytes and pericytes differentially modulate blood-brain barrier characteristics during development and hypoxic insult. *J Cereb Blood Flow Metab* 2011; **31**: 693–705.
- Fukushi J, Makagiansar IT, Stallcup WB. NG2 proteoglycan promotes endothelial cell motility and angiogenesis via engagement of galectin-3 and alpha3beta1 integrin. *Mol Biol Cell* 2004; **15**: 3580–3590.
- Hill JW, Poddar R, Thompson JF, Rosenberg GA, Yang Y. Intranuclear matrix metalloproteinases promote DNA damage and apoptosis induced by oxygen-glucose deprivation in neurons. *Neuroscience* 2012; **220**: 277–290.
- McColl BW, Rothwell NJ, Allan SM. Systemic inflammation alters the kinetics of cerebrovascular tight junction disruption after experimental stroke in mice. *J Neurosci* 2008; **28**: 9451–9462.
- Rosell A, Cuadrado E, Ortega-Aznar A, Hernandez-Guillamon M, Lo EH, Montaner J. MMP-9-positive neutrophil infiltration is associated to blood-brain barrier breakdown and basal lamina type IV collagen degradation during hemorrhagic transformation after human ischemic stroke. *Stroke* 2008; **39**: 1121–1126.
- Xing C, Levchenko T, Guo S, Stins M, Torchilin VP, Lo EH. Delivering minocycline into brain endothelial cells with liposome-based technology. *J Cereb Blood Flow Metab* 2012; **32**: 983–988.
- Ahn SM, Byun K, Kim D, Lee K, Yoo JS, Kim SU et al. Olig2-induced neural stem cell differentiation involves downregulation of Wnt signaling and induction of Dickkopf-1 expression. *PLoS ONE* 2008; **3**: e3917.
- Yang Y, Jalal FY, Thompson JF, Walker EJ, Candelario-Jalil E, Li L et al. Tissue inhibitor of metalloproteinases-3 mediates the death of immature oligodendrocytes via TNF-alpha/TACE in focal cerebral ischemia in mice. *J Neuroinflammation* 2011; **8**: 108–122.

Supplementary Information accompanies the paper on the Journal of Cerebral Blood Flow & Metabolism website (<http://www.nature.com/jcbfm>)